文章编号:1006-9941(2019)08-0685-07

Research on Thermal Decomposition of Dihydroxylammonium 5,5′-Bistetrazole-1,1′-diolate (TKX-50) by Decoupling Method

ZHU Yan-long, AN Jing, DING Li, BI Fu-qiang, ZHOU Jing, LIANG Yi

(*Xi′ an Modern Chemistry Research Institute, Xi′an* 710065, *China*)

Abstract: To study the thermal decomposition of dihydroxylammonium 5,5′-bistetrazole-1,1′-diolate (TKX-50), thermal decomposition experiments such as thermogravimetry and differential scanning calorimetry were carried out, respectively. Meanwhile, MATLAB software was employed to decouple the overlapping parts and the Málek method was used to study the kinetics of the thermal decomposition of TKX-50. The results show that the thermal decomposition process of TKX-50 is divided into two stages. The complete thermal decomposition curves of the two stages are obtained by MATLAB software, and the basic parameters such as T_{onset}, T_p, and ΔH are acquired at different heating rates. The thermal decomposition of TKX-50 follows the autocatalytic reaction model, and the kinetic parameters including activation energy, pre-exponential factor and kinetic model are obtained, respectively. For the first stage, E_a=174.99 kJ·mol^{-1}, ln$A$=40.75, $f(\alpha)=\alpha^{0.917}(1-\alpha)^{0.509}$, for the second stage, E_a=149.60 kJ·mol^{-1}, ln$A$=31.84, $f(\alpha)=\alpha^{0.357}(1-\alpha)^{0.117}$.

Key words: dihydroxylammonium 5,5′-bistetrazole-1,1′-diolate (TKX-50); decoupling; thermal decomposition; Málek method

CLC number: TJ55; O65 **Document code:** A **DOI:** 10.11943/CJEM2018335

1 Introduction

Tetrazoles are considered to be the promising candidate for high energy density material (HEDM) because of a large number of energetic N—N bond and C—N bond, strong ring strain, high density, high enthalpy of formation, a big amount of gas generation, low sensitivity, good thermal stability and environmentally friendly products of detonation[1-3]. It has caused great attention of many scholars[4-5].

As a typical representative of tetrazoles, dihydroxylammonium 5, 5′-bistetrazole-1, 1′-diolate (TKX-50) has the density of 1.918 g·cm^{-3}, theoretical detonation velocity of 9698 m·s^{-1}, energy level approaching that of hexanitrohexaazaisowurtzitane (CL-20) and sensitivity of lower than HMX and RDX, thus, it is considered as an energetic compound which has excellent comprehensive performance[6].

Currently, there is much research[7-9] on the application of TKX-50. It is well known that thermal analysis study of energetic materials (EMs) is important not only for understanding of the kinetics of their thermal decomposition but also for assessing the effect of their exothermic decomposition on the potential hazardous in their handling, processing and storage. Kinetic studies also provide useful information[10-12] on the thermal stability and life expectancy (reliability) of EMs under different thermal environment in storage.

It is reported that the thermal decomposition process of TKX-50 is divided into two steps, which overlaps with each other[13-20]. However, there is no detailed and further investigation dealing with the real process of each stage. In this work, the overlapping parts in the thermal decomposition were suc-

Received Date: 2018-12-03; **Revised Date:** 2019-03-17

Published Online: 2019-04-01

Project Supported: The National Natural Science Foundation of China (21503162 and 21805226)

Biography: ZHU Yan-long (1988-), male, engineer, research fields: thermal analysis and thermal safety of energetic materials. e-mail: zhuyanlong523@126.com

Corresponding author: DING Li (1971-), female, professor, research fields: thermal analysis and thermal safety of energetic materials. e-mail: dingli403@sina.com

引用本文: 祝艳龙,安 静,丁 黎,等. 解耦合法研究1,1′-二羟基-5,5′-联四唑二羟胺盐(TKX-50)热分解[J]. 含能材料,2019,27(8):685-691.

ZHU Yan-long, AN Jing, DING Li, et al. Research on Thermal Decomposition of Dihydroxylammonium 5,5′-Bistetrazole-1,1′-diolate (TKX-50) by Decoupling Method[J]. *Chinese Journal of Energetic Materials (Hanneng Cailiao)*, 2019, 27(8): 685-691.

cessfully decoupled by mathematical methods and the thermal decomposition kinetics of each stage was studied. Meanwhile, the Málek method was employed to fit the most probable mechanism of each stage, respectively. This study can provide a guidance for the application in handling, processing and storage of EMs.

2 Experimental

2.1 Materials

TKX-50 was supplied by Xi'an Modern Chemistry Research Institute, recrystallized from water and had a purity of more than 99.5% through liquid chromatography (LC). The structure of TKX-50 was shown in Fig. 1. ^{1}H NMR (500 MHz, DMSO-d_6) δ: 10.18(8H, N—H and O—H); ^{13}C NMR(125 MHz, DMSO-d_6) δ: 134.98. IR(KBr, ν/cm^{-1}): 3221, 3084, 2913, 2682, 2504, 1578, 1526, 1427, 1413, 1351, 1236, 1172, 1133, 1045, 1011, 997, 814, 716, 674, 499. Anal. Calcd. for $C_2H_8N_{10}O_4$(%): C 10.17, H 3.41, N 59.31, found(%): C 10.05, H 3.39, N 59.56. MS (ESI), m/z: 168.59 $[C_2N_8O_2]^{2-}$.

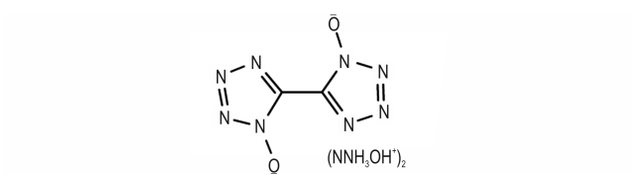

Fig.1 Structure of TKX-50[6]

2.2 Equipments and Conditions

The tests of DSC and TG were made by the DSC-TG coupling technique on a 449C thermal analyzer (NETZSCH, Germany). The heating rates were 2.5, 5, 10, 20 ℃·min^{-1} from ambient temperature to 400 ℃ in the test of decomposition kinetics. All experiments were carried out in a nitrogen atmosphere at a rate of 50 mL·min^{-1}. The amount of samples used for the each test was about 0.5 mg.

3 Results and Discussions

3.1 Thermal Decomposition Behavior of TKX-50

On the TG curve in Fig. 2, initial sample mass loss of 99.87% at 186.68 ℃ is due to the evaporation of water or/and solvent. Temperature is 223.98 ℃ when mass loss is 5%, T_d is 223.98 ℃. It is obvious that the thermal decomposition in two stages. The mass loss is about 52% in the first stage and about 20% in the second stage where decomposition reacts slightly slow, resulting in about 23% solid residue at the end. Meanwhile, it can be seen from the DTG curve that there are an overlapping part in two decomposition stages.

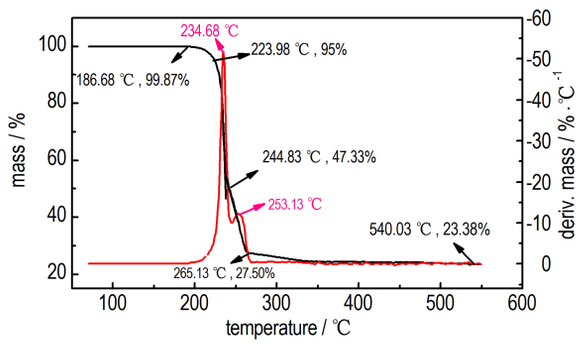

Fig. 2 TG and DTG curves of TKX-50 at a heating rate of 10 ℃·min^{-1}

The same conclusion appears on the DSC curves in Fig. 3. It can be clearly seen that the thermal decomposition in two stages. The narrow, sharp exothermic peaks appear between 220–260 ℃, which indicates that the first decomposition stage is very fast, while the second decomposition stage corresponds to a slower completion of the decomposition reaction. At the same time, the two decomposition stages have overlapping parts.

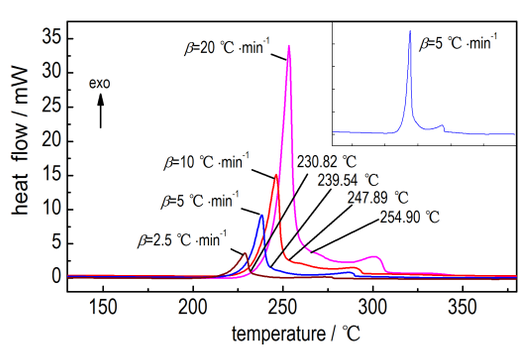

Fig.3 DSC curves of TKX-50 at different heating rates

3.2 Decoupling of Two Stages in Decomposition by Mathematical Method

There are obvious coupling parts in the range of 230–280 ℃ on the DSC curves of TKX-50 under different heating rates. There is an inflection point after

the first decomposition peak, as shown in Fig.3. In order to study the thermal decomposition of each stage, the coupling parts of two stages are separated by MATLAB software. Then the first stage of the thermal decomposition are fitted until the inflection point using MATLAB software's curve fitting tool (Fig. 4). There are 10 function options available, such as Gaussian, polynomial, power, exponential, Fourier functions, and so on, among which the Gaussian function is the best fitting function[21], resulting in a uniform mathematical expression shown as Eq.(1), between heat flow and temperature, where y represents the heat flow, and x represents temperature. a_n, b_n, c_n(n=1, 2, 3, 4)are the constant of the equation depending on the heating rates. All of the above-mentioned parameters are listed in Table 1. Thus, the complete decomposition curves of the first stage of thermal decomposition are obtained. The complete second stage of the thermal decomposition curves are obtained by subtracting the first stage of the thermal decomposition curves from the DSC curves (Fig. 4). The characteristic parameters of the thermal decomposition process obtained from two complete thermal decomposition curves are shown in Table 2, from which we can get the onset temperature, the peak temperature, the enthalpy of decomposition reaction of each stage. All of these parameters will provide guidance for production, handling, storage, simulation and calculation of TKX-50[11-12].

$$y=a_1e^{-(x-b_1/c_1)^2}+a_2e^{-(x-b_2/c_2)^2}+a_3e^{-(x-b_3/c_3)^2}+a_4e^{-(x-b_4/c_4)^2} \quad (1)$$

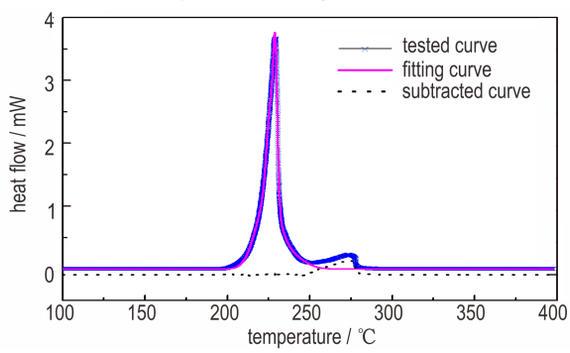

Fig.4 Tested curve, fitting curve and subtracted curve at a heating rate of 2.5 ℃·min^{-1}

Table 1 Fitting parameters by MATLAB at different heating rates

β/℃·min^{-1}	a_1	b_1	c_1	a_2	b_2	c_2	a_3	b_3	c_3	a_4	b_4	c_4
2.5	1.858	229.1	1.696	1.523	226.5	3.497	1.081	224.3	9.989	0.1867	238.9	11.45
5	4.263	238.5	1.367	4.145	236.4	2.881	2.736	233.9	8.132	0.4672	247.6	9.39
10	6.398	245.0	2.595	3.023	241.5	4.658	5.937	247.0	1.534	3.877	243.4	11.48
20	13.85	253.7	1.424	15.49	251.8	3.419	9.96	249.8	9.474	1.13	258.1	1.593

Table 2 The characteristic parameters of the thermal decomposition

β / ℃·min^{-1}	the first stage			the second stage		
	T_{onset} /℃	T_p / ℃	$-\Delta H$ / J·g^{-1}	T_{onset} / ℃	T_p / ℃	$-\Delta H$ / J·g^{-1}
2.5	219.55	229.07	1776.28	248.40	273.33	199.84
5	229.85	238.25	1792.71	267.20	280.60	199.40
10	236.50	246.25	1783.50	275.06	289.597	200.00
20	244.73	253.48	1750.22	283.28	301.597	199.71
average			1775.68			199.74

Note: β is the heating rate, T_{onset} is the onset temperature, T_p is the peak temperature, ΔH is the enthalpy of decomposition reaction.

3.3 Non-isothermal Kinetics of Thermal Decomposition of TKX-50

3.3.1 Theoretical Backgrounds

In the study of thermal decomposition kinetics, activation energy (E_a), pre-exponential factor (A), and kinetic model $f(\alpha)$ of each stage need to be determined. E_a is generally used to obtain by model-free isoconversional methods, which can ignore the impact from the different kinetic models. To solve the kinetic model, Málek[22-25] suggests using a classic algorithm (Scheme 1) based on the shape and the extreme values of the characteristic function

$y(\alpha)$ and $Z(\alpha)$, which are obtained by a simple transformation of experimental data. The most suitable kinetic model is then acquired based on both the conversion degree $\alpha_{max,y}$ corresponding to the maximum of the $y(\alpha)$ function and $\alpha_{max,z}$, which corresponds to the maximum of the $Z(\alpha)$ function. Finally, the pre-exponential factor is obtained from the mechanism function.

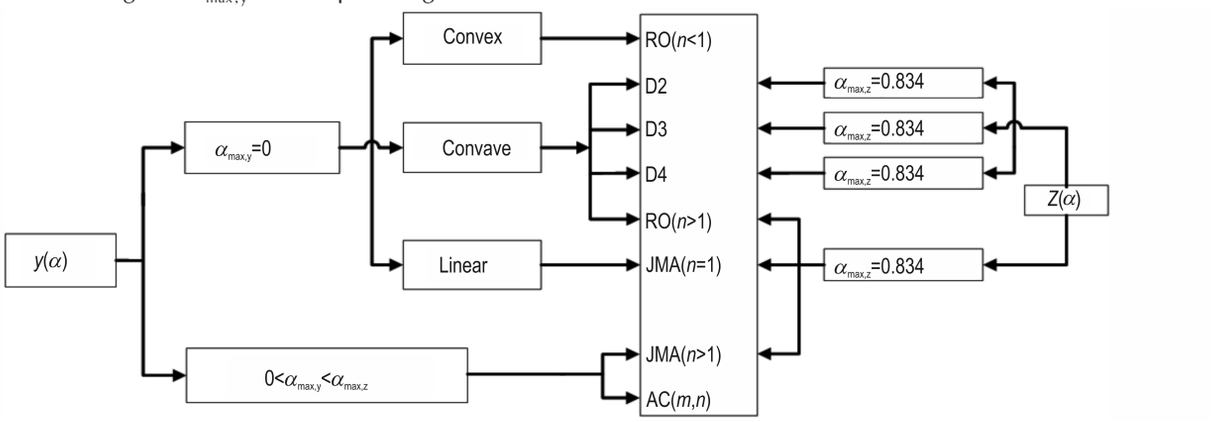

Scheme 1 Determine the flow diagram of the mechanism function

3.3.2 Acquirement of Activation Energy

In this paper, the activation energy is obtained by using the Ozawa method[26] at the same conversion, shown as Eq.(2).

$$\lg\beta = \lg\left[\frac{AE_a}{RG(\alpha)}\right] - 2.315 - \frac{0.4567E_a}{RT} \quad (2)$$

Where β is the heating rate, ℃·min^{-1}; A is the pre-exponential factor, s^{-1}; E_a is the activation energy, kJ·mol^{-1}; R is the standard gas constant, 8.314 J·K^{-1}·mol^{-1}; α is the conversion, $G(\alpha)$ is the integral form of kinetic function, T is the Kelvin temperature, K. The relationship between lg β and 1/T is a straight line. The activation energy can be determined from the slope of this line at each conversion. Combined Eq.(2) and the integration of heat flow curves(Fig.4), the relationship between E_a and α is displayed in Fig.5. As can be seen from Fig.5, the average activation energy of TKX-50 in two stages are substantially steady, ranging from 168.6 kJ·mol^{-1} to 179.4 kJ·mol^{-1} when the conversion is 0.15−0.80 in the first stage, 140.8 kJ·mol^{-1} to 158.3 kJ·mo^{-1} when the conversion is 0.10−0.85 in the second stage. It implies that the decomposition of TKX-50 in each stage is presented in a single-step reaction, which can be described with a single mechanism function. At the same time, the average activation energy of each stage is obtained from the results of Fig. 5, which values are 174.99 kJ·mol^{-1} and 149.60 kJ·mol^{-1}, respectively.

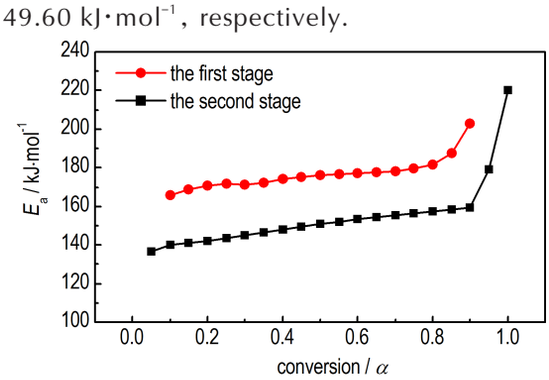

Fig.5 The relationships between E_a and α in the thermal decomposition

3.3.3 Mechanism Function

In this paper, the most suitable kinetic model $f(\alpha)$ are determined by the shape and the extreme values ($\alpha_{max,y}$ and $\alpha_{max,Z}$) of the characteristic functions $y(\alpha)$ and $Z(\alpha)$. The function expression of $y(a)$ and $Z(\alpha)$ are shown as Eq.(3) and (4). The function expression of $\pi(u)$ in Eq.(4) using its third-order expansion[27] according to experience, is shown as Eq.(5) and u=E_a/RT.

$$y(\alpha) = \left(\frac{T}{T_{0.5}}\right)^2 \frac{\frac{d\alpha}{dt}}{\left(\frac{d\alpha}{dt}\right)_{0.5}} = \frac{f(\alpha)\times G(\alpha)}{f(0.5)\times G(0.5)} \quad (3)$$

$$Z(\alpha) = \frac{\pi(u)\times\frac{d\alpha}{dt}\times T}{\beta} = f(\alpha)\times G(\alpha) \quad (4)$$

$$\pi(u)=\frac{u^2+10u+18}{u^3+12u^2+36u+24} \quad (5)$$

$$f(\alpha)=\alpha^m(1-\alpha)^n \quad (6)$$

$$\frac{m}{n}=\frac{\alpha_{\max,y}}{1-\alpha_{\max,y}} \quad (7)$$

$$\ln\left[\left(\frac{\mathrm{d}\alpha}{\mathrm{d}t}\right)\exp\left(\frac{E_a}{RT}\right)\right]=\ln A+n\times\ln\left[\alpha^{m/n}(1-\alpha)\right] \quad (8)$$

Combined Eqs.(3)-(5), experimental data α_i, T_i, $(\mathrm{d}\alpha/\mathrm{d}t)_i$ (i=1, 2, …, j), and α=0.5, $T_{0.5}$, $(\mathrm{d}\alpha/\mathrm{d}t)_{0.5}$ are substituted into Eq.(3) and the $y(\alpha)-\alpha$ curves are displayed in Figs.6 and 7. Meanwhile, the average activation energy E_a, T_i, $(\mathrm{d}\alpha/\mathrm{d}t)_i$ and β_i are substituted into Eq.(4) and the $Z(\alpha)$-α curves are displayed in Figs. 6 and 7. The extreme values ($\alpha_{\max,y}$, $\alpha_{\max,Z}$) of the $y(\alpha)$-α curves and the $Z(\alpha)$-α curves are obtained after fitted by polynomial. The results are shown in Table 3.

According to the shape and the extreme values ($\alpha_{\max,y}$, $\alpha_{\max,Z}$) of the characteristic functions $y(\alpha)$ and $Z(\alpha)$, the most suitable kinetic model is AC reaction model: $f(\alpha)=\alpha^m(1-\alpha)^n$ on the basis of Scheme 1. That is to say, the kinetic model of each stage in the decomposition reaction follows the autocatalytic reaction model.

The parameters m, n in the AC reaction model are acquired by Eqs.(7) and (8). The pre-exponential factor is also obtained by linear fitting through Eq.(8). All of the parameters for decomposition reaction models of TKX-50 are listed in Table 4. Finally, the most suitable kinetic model for each stage of decomposition reaction of TKX-50 is $f(\alpha)=\alpha^{0.917}(1-\alpha)^{0.509}$ and $f(\alpha)=\alpha^{0.357}(1-\alpha)^{0.117}$, respectively.

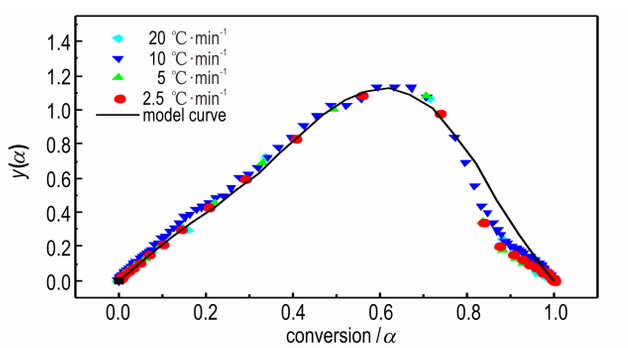

a. $y(\alpha)$-α

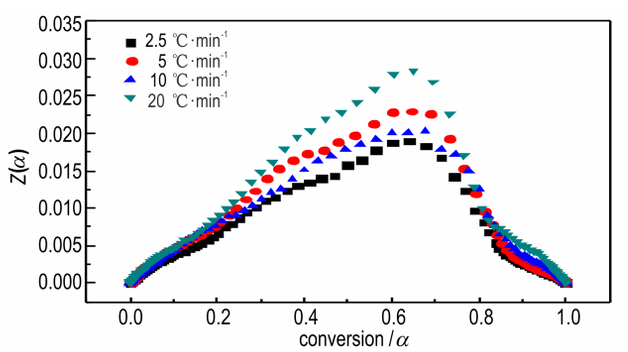

b. $Z(\alpha)$-α

Fig.6 The relationships between $y(\alpha)$, $Z(\alpha)$ and α at the first stage of thermal decomposition

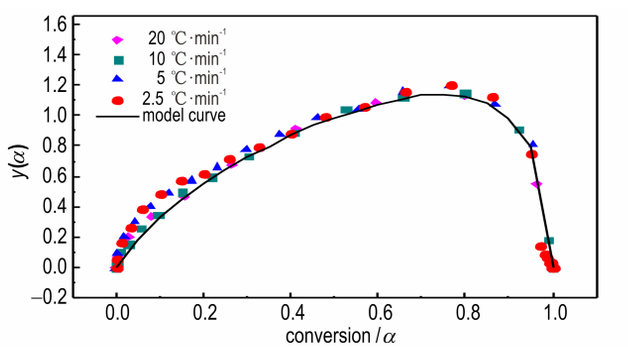

a. $y(\alpha)$-α

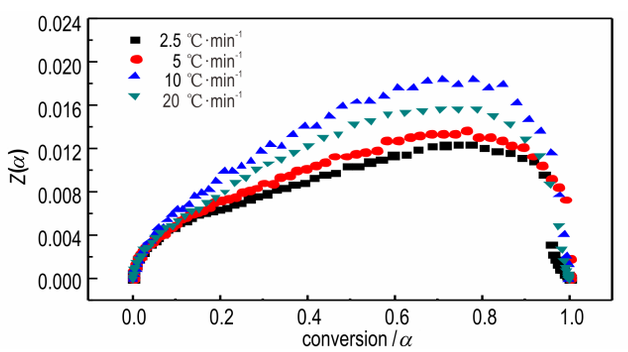

b. $Z(\alpha)$-α

Fig.7 The relationships between $y(\alpha)$, $Z(\alpha)$ and α in the second stage

Table 3 Kinetic parameters of each stage in thermal decomposition

	β	$\alpha_{\max,y}$	$\alpha_{\max,Z}$	Model	m	n	E_a	ln$A$
First stage	2.5-20	0.643	0.643	AC	0.917	0.509	174.99	40.75
Second stage	2.5-20	0.753	0.753	AC	0.357	0.117	149.60	31.84

4 Conclusions

(1) The thermal decomposition of TKX-50 can be divided into two stages, and there were obvious coupling parts in the range of 230−280 ℃ on the DSC curves at different heating rates.

(2) The coupling parts of the two stages of thermal decomposition were decoupled by MATLAB software. Then the complete decomposition curves of each stage of TKX-50 were obtained.

(3) The thermal decomposition kinetics of each stage was studied by Málek method, the activation energy (E_a), pre-exponential factor (A), and kinetic model $f(\alpha)$ of each stage was obtained, for the first stage, E_a=174.99 kJ·mol^{-1}, ln$A$=40.75, $f(\alpha)=\alpha^{0.917}(1-\alpha)^{0.509}$, for the second stage, E_a=149.60 kJ·mol^{-1}, ln$A$=31.84, $f(\alpha)=\alpha^{0.357}(1-\alpha)^{0.117}$, which can support the using of TKX-50 in handling, processing and storage.

References:

[1] Chavez D E, Hiskey M A, Gilardi R D. 3,3′-Azobis(6-amino-1,2,4,5-tetrazine): a novel high-nitrogen energetic material [J]. *Angewandte Chemie-International Edition*, 2000, 39(10): 1791−1793.

[2] Xue H, Gao H X, Twamley B, et al. Energetic nitrate, perchlorate, azide and azolate salts of hexamethylenetetramine [J]. *European Journal of Inorganic Chemistry*, 2006, 15: 2959−2965.

[3] Rossi R A, Pierini A B, Penenory A B. Nucleophilic substitution reactions by electron transfer [J]. *Chemical Reviews*, 2003, 103(1): 71−167.

[4] Strout D L. Stability of carbon-nitrogen cages in fourfold symmetry [J]. *Journal of Physical Chemistry A*, 2006, 110(11): 4089−4092.

[5] BI Fu-qiang, FAN Xue-zhong, XU Cheng, et al. Review on insensitive non-metallic energetic ionic compounds of tetrazolateanions [J]. *Chinese Journal of Energetic Materials* (*Hanneng Cailiao*), 2012, 20(6): 805−811.

[6] Fischer N, Fischer D, Klapotke T M, et al. Pushing the limits of energetic materials - the synthesis and characterization of dihydroxylammonium 5,5′-bistetrazole-1,1′-diolate [J]. *Journal of Materials Chemistry*, 2012, 22(38): 20418−20422.

[7] Huang H F, Shi Y M, Yang J, et al. Compatibility study of dihydroxylammonium 5, 5′-bistetrazole-1, 1′-diolate (TKX-50) with some energetic materials and inert materials [J]. *Journal of Energetic Materials*, 2015, 33(1): 66−72.

[8] Li N, Zhao F Q, Luo Y, et al. Dissolution thermokinetics of dihydroxylammonium 5,5′-bistetrazole-1,1′-diolate in dimethyl sulfoxide [J]. *Journal of Thermal Analysis and Calorimetry*, 2015, 122(2): 1023−1027.

[9] Dreger Z A, Stash A I, Yu Z G, et al. High-pressure structural response of an insensitive energetic crystal: dihydroxylammonium 5, 5′-bistetrazole-1, 1′-diolate (TKX-50) [J]. *Journal of Physical Chemistry C*, 2017, 121(10): 5761−5767.

[10] Zhang J Q, Gao H X, Ji T Z, et al. Non-isothermal decomposition kinetics, heat capacity and thermal safety of 37.2/44/16/2.2/0.2/0.4-GAP/CL-20/Al/N-100/PCA/auxiliaries mixture [J]. *Journal of Hazardous Materials*, 2011, 193(5): 183−187.

[11] Yi J H, Zhao F Q, Wang B Z, et al. Thermal behaviors, non-isothermal decomposition reaction kinetics, thermal safety and burning rates of BTATz-CMDB propellant [J]. *Journal of Hazardous Materials*, 2010, 181(1−3): 432−439.

[12] Xu K Z, Song J R, Zhao F Q, et al. Thermal behavior, specific heat capacity and adiabatic time-to-explosion of G(FOX-7) [J]. *Journal of Hazardous Materials*, 2008, 158(2−3): 333−339.

[13] Sinditskii V P, Filatov S A, Kolesov V I, et al. Combustion behavior and physico-chemical properties of dihydroxylammonium 5,5′-bistetrazole-1,1′-diolate (TKX-50) [J]. *Thermochimica Acta*, 2015, 614(1): 85−92.

[14] Yuan B, Yu Z J, Bernstein E R. Initial mechanisms for the decomposition of electronically excited energetic salts: TKX-50 and MAD-X1 [J]. *Journal of Physical Chemistry A*, 2015, 119(12): 2965−2981.

[15] Ma S, Li Y J, Li Y, et al. Research on structures, mechanical properties, and mechanical responses of TKX-50 and TKX-50 based PBX with molecular dynamics [J]. *Journal of Molecular Modeling*, 2016, 22(2): 43.

[16] Huang H F, Shi Y M, Yang J. Thermal characterization of the promising energetic material TKX-50 [J]. *Journal of Thermal Analysis and Calorimetry*, 2015, 121(2): 705−709.

[17] Niu H, Chen S S, Jin S H, et al. Thermolysis, nonisothermal decomposition kinetics, calculated detonation velocity and safety assessment of dihydroxylammonium 5,5′-bistetrazole-1,1′-diolate [J]. *Journal of Thermal Analysis and Calorimetry*, 2016, 126(2): 473−480.

[18] Lesnikovich A I, Ivashkevich O A, Printsev G V, et al. Thermal decomposition of tetrazolepart III. Analysis of decomposition products [J]. *Thermochimica Acta*, 1990, 171: 207−213.

[19] An Q, Liu W G, Goddard W A, et al. Initial steps of thermal decomposition of dihydroxylammonium 5, 5′-bistetrazole-1, 1′-diolate crystals from quantum mechanics [J]. *Journal of Physical Chemistry C*, 2014, 118(46): 27175−27181.

[20] An Q, Cheng T, Goddard W A, et al. Anisotropic impact sensitivity and shock induced plasticity of TKX-50 (dihydroxylammonium 5, 5′-bis (tetrazole)-1, 1′-diolate) single crystals: from large-scale molecular dynamics simulations [J]. *Journal of Physical Chemistry C*, 2015, 119(4): 2196−2207.

[21] Zhang C X, Lu G B, Chen L P, et al. Two decoupling methods for non-isothermal DSC results of AIBN decomposition [J]. *Journal of Hazardous Materials*, 2015, 285: 61−68.

[22] Málek J. The kinetic-analysis of nonisothermaldata [J]. *Thermochimica Acta*, 1992, 200: 257−269.

[23] Málek J. Kinetic analysis of crystallization processes in amorphous materials [J]. *Thermochimica Acta*, 2000, 355(1−2): 239−253.

[24] Málek J, Criado J M. Is the Sestak-Berggren equation a general expression of kinetic-models [J]. *Thermochimica Acta*, 1991, 175(2): 305−309.

[25] Svoboda R, Málek J. Interpretation of crystallization kinetics results provided by DSC[J]. *ThermochimicaActa*, 2011, 526(1-2): 237-251.

[26] Ozawa T. A new method of analyzing thermogravimetricdata [J]. *Bulletin of the Chemical Society of Japan*, 1965, 38(11): 1881-1886.

[27] HU Rong-zu, GAO Sheng-li, ZHAO Feng-qi, et al. Thermal Analysis Kinetics(2th)[M]. Beijing: Science Press, 2008: 149-165.

解耦合法研究1,1′-二羟基-5,5′-联四唑二羟胺盐(TKX-50)热分解

祝艳龙,安 静,丁 黎,毕福强,周 静,梁 忆
(西安近代化学研究所, 陕西 西安 710065)

摘 要: 为了研究1,1′-二羟基-5,5′-联四唑二羟胺盐(TKX-50)的热分解,分别采用热重和差示扫描量热法进行热分解试验研究,并采用MATLAB软件对重合部分进行解耦合,用Málek方法对TKX-50热分解过程进行动力学研究。结果表明,TKX-50的热分解过程分为两个阶段,用MATLAB 软件获得两个阶段完整的热分解曲线,并分别获得不同升温速率下各个阶段的T_{onset}、T_p、ΔH等基础参数。TKX-50的热分解遵循自催化反应模型,并分别获得动力学参数包括活化能、指前因子和动力学模型等,第一阶段:E_a=174.99 kJ·mol^{-1},ln$A$=40.75,$f(\alpha)=\alpha^{0.917}(1-\alpha)^{0.509}$;第二阶段:$E_a$=149.60 kJ·mol^{-1},ln$A$=31.84,$f(\alpha)=\alpha^{0.357}(1-\alpha)^{0.117}$。

关键词: 1,1′-二羟基-5,5′-联四唑二羟胺盐(TKX-50);解耦合;热分解;Málek方法

中图分类号: TJ55; O65 **文献标志码:** A **DOI:** 10.11943/CJEM2018335

(责编:高 毅)